Journal of proteome research

pubs.acs.org/jpr Article

Impact of PPP1R1A Knockdown on the Proteomic Landscape of INS-1 Cells: A Focus on Significant Modulated Pathways

Published as part of Journal of Proteome Research special issue "Multiomics in Africa and the Middle East".

Jalal Taneera,* Alexander D. Giddey, Nelson C. Soares, Anila Khalique, Abdul Khader Mohammed, Mohamed Omer Mahgoub, and Eglal Mahgoub*

Cite This: J. Proteome Res. 2026, 25, 460−470 Read Online

ACCESS | Metrics & More | Article Recommendations | Supporting Information

ABSTRACT: PPP1R1A (protein phosphatase 1 regulatory inhibitor subunit 1A) is a cAMP/PKA-responsive inhibitor of protein phosphatase 1 (PP1) with a pivotal role in pancreatic β-cell physiology. To investigate its functional impact, Ppp1r1a was silenced in INS-1 (832/13) rat β-cells, and proteomic alterations were profiled using label-free DIA mass spectrometry (Orbitrap Exploris 480) with a rat spectral library. Quantitative analysis (n = 4/group) identified ~2846 proteins with >2-fold change, revealing extensive proteome reprogramming. Key biological processes affected included vesicle trafficking and exocytosis, insulin biosynthesis and processing, organelle organization, mRNA processing, and autophagy. Pathway enrichment highlighted disruptions in insulin secretion, insulin resistance, and mTOR signaling. Crucial β-cell proteins, including INS2, Cacna1a, CPEB2, PCSK2, SNAP25, SYT5, and VAMP7, were significantly downregulated. Validation confirmed reduced phosphorylated AKT levels and p-AKT/T-AKT ratio, consistent with impaired mTOR signaling. Collectively, these findings demonstrate that PPP1R1A is essential for maintaining β-cell function and insulin secretion, and its depletion triggers broad proteomic and signaling alterations. Thus, PPP1R1A emerges as a regulatory node with potential therapeutic relevance in modulating β-cell activity and insulin dynamics in diabetes.

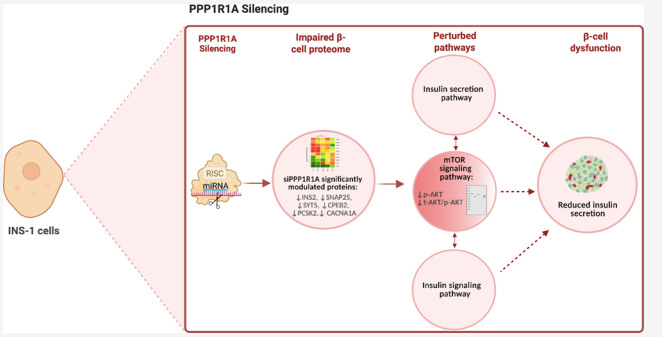

KEYWORDS: *PPP1R1A, proteomics, insulin secretion, pancreatic β-cells, mTOR signaling, AKT phosphorylation*

INTRODUCTION

PPP1R1A, also known as protein phosphatase 1 regulatory inhibitor subunit 1A, is a crucial regulatory protein that plays a pivotal role in various cellular processes, including metabolism, cell division, and signal transduction. This protein primarily functions as an inhibitor of protein phosphatase 1 (PP1), a major serine/threonine phosphatase responsible for dephosphorylating numerous substrates involved in critical signaling pathways.[1]

By regulating PP1 activity, PPP1R1A influences diverse physiological functions, including muscle contraction, neuronal signaling, and insulin secretion. Dysregulation of PPP1R1A has been implicated in several diseases, including type 2 diabetes, cardiovascular diseases, and certain cancers, underscoring its significance in maintaining cellular homeostasis and overall metabolic health.[2−5] Due to its regulatory functions, PPP1R1A is a potential target for therapeutic interventions aimed at restoring normal cellular function in pathological conditions.[6]

Our previous research demonstrated that disruption of PPP1R1A in INS-1 cells led to decreased insulin secretion and impaired glucose uptake, accompanied by significant downregulation of key β-cell function genes, including Ins1, Ins2, Pcsk1, Pdx1, Mafa, and components of the exocytosis and calcium transport machinery.[7] Importantly, cell viability, reactive oxygen species levels, apoptosis, and proliferation remained unaffected, indicating a specific impact on β-cell functional pathways. Additionally, we found that PDX1 regulates PPP1R1A expression and can be upregulated by rosiglitazone treatment. Building upon these findings, our current proteomics analysis serves as a continuation to further elucidate the molecular mechanisms by which PPP1R1A modulates β-cell function and insulin secretion. We examined the downstream proteins involved in the signaling pathways affected in our proteomics analysis. These findings were subsequently validated by Western blotting, which corrobo-

Received: October 7, 2025
Revised: November 18, 2025
Accepted: November 27, 2025
Published: December 8, 2025

https://doi.org/10.1021/acs.jproteome.5c00889
J. Proteome Res. 2026, 25, 460−470

rated the alterations in key pathway components, thereby strengthening the evidence of PPP1R1A's regulatory impact on β-cell molecular networks.

METHODS

Cell Line and Cell Culture

The rat insulinoma INS-1 (832/13) cell line was obtained from AddexBio (San Diego, CA, USA). Cells were cultured in RPMI 1640 medium supplemented with 10% (v/v) heat-inactivated fetal bovine serum (FBS), 2 mM L-glutamine, 1 mM sodium pyruvate, 10 mM HEPES, 50 μM β-mercaptoethanol, 100 U/mL penicillin, and 100 μg/mL streptomycin. Cultures were maintained at 37 °C in a humidified incubator with 5% CO_2.[7]

Transfection siRNA

Small interfering RNAs (siRNAs) targeting Ppp1r1a (Cat. No. s131449 and s131450), siRNA negative control and Lipofectamine 3000, were obtained from Thermo-Fisher Scientific (USA). For Ppp1r1a gene silencing, transfections were conducted with a pooled mixture of both siRNA sequences at a final concentration of 40 nM to optimize silencing efficiency and target specificity.[7]

Western Blotting

M-PER, Mammalian protein extraction reagent (Thermo-Fisher Scientific, USA), containing a protease inhibitor cocktail. Protein quantification was performed using the Bradford Assay. A volume equivalent to 30 μg of total protein was separated on a 10% sodium dodecyl sulfate-polyacrylamide gel electrophoresis (SDS-PAGE) gel, which was then electrophoretically transferred to a PVDF membrane (Bio-Rad, USA). The membrane was blocked for 1 h at room temperature using 5% BSA powder.

Following blocking, the membrane was washed with TBST and incubated overnight at 4 °C with primary antibodies, including anti-PPP1R1A (Cat. No. ab40877, Abcam, Cambridge, UK), anti-Akt (Cat. No. 9272, Cell Signaling Technology, Massachusetts, USA), antiphospho-Akt (p-Akt) (Cat. No. 12694, Cell Signaling Technology, Massachusetts, USA), anti-β-actin (Cat. No. 4970, Cell Signaling Technology, Massachusetts, USA), overnight at 4 °C. Secondary antibodies antimouse IgG (Cat. No. 7076S:2500, Cell Signaling Technology, Massachusetts, USA) and antirabbit IgG (Cat. No. 7074S; 1:2500, Cell Signaling Technology, Massachusetts, USA) were incubated with the membrane for 1 h at room temperature at a ratio of 1:1000. The ECL kit (Thermo Scientific Pierce, Waltham, MA, USA) was used to identify chemiluminescence to identify and quantify protein bands, Bio-Rad Image Lab software (ChemiDocTM Touch Gel and Western Blot Imaging System; Bio-Rad, Hercules, CA, USA) was used. Protein levels were normalized to β-actin, and ratios were calculated based on the values of control samples.

Proteomics Sample Processing

Frozen Cell pellets were prepared for LC-MS analysis by way of the SPEED (Sample Preparation by Easy Extraction and Digestion) method.[8] Briefly, 20 μL trifluoroacetic acid (TFA) was added to each cell pellet and allowed to dissolve completely at 70 °C for 10 min. Samples were neutralized by the addition of 200 μL 2 M Tris-base, reduced, and alkylated by way of 1 mM dithiothreitol (DTT) and 5.5 mM iodoacetamide (IAA) for 1 h and 30 min, respectively. OD360 readings were used to normalize sample concentrations, and ∼100 μg of sample was taken for digestion. Digestion by LysC/Trypsin combination was carried out at 37 °C for 20 h at an enzyme: sample ratio of 1:100. Digestion was stopped by acidification, and samples STAGE tipped, dried, and resolubilized in 100 μL 2% acetonitrile prior to LC-MS analysis.

LC-MS Analysis

Samples were analyzed using a Vanquish Neo chromatography setup in line with an Orbitrap Exploris 480 mass spectrometer. Injection volumes were calculated based on preliminary runs to normalize total protein abundance. Samples were separated along a 1.5 h gradient using a 50 cm EasySpray C18 column maintained at 50 °C. The procedure was as follows: the column was equilibrated to 4% B at a flow rate of 600 nL/min prior to the gradient start, and the flow rate then dropped to 250 nL/min. Gradient elution occurred from 4% B to 20% B over 60 min, followed by a 25 min increase to 35% B. A final elution was performed at 55% B over 2 min, followed by the cessation of MS acquisition and the initiation of a sequence of washing steps. Solvent A was 0.1% formic acid in water, and solvent B was 80% acetonitrile, 0.1% formic acid.

Data acquisition was performed using data-independent acquisition in positive mode. Full MS1 scans, from 380 to 985 m/z, were acquired every 3 s at 120,000 resolution, and DIA MS2 scans were acquired from 145 to 1450 m/z at 60,000 resolution with 59 custom-width MS1 windows as defined in the supplementary data.

Proteomics Data Processing and Statistical Analysis

Samples were converted to the open mzML format using msconvert[8] and then processed with DIA-NN[9] version 1.8.1. The spectral library was the DIA-NN in-silico predicted spectral library, built using the UniProt reference (UP000002494). The spectral library was generated with default settings, allowing for one missed cleavage and no variable modifications. Samples were processed with mass accuracy set to 10 ppm, heuristic protein inference turned off, match-between-runs on and neural network classifier set to double-pass mode. Precursors were filtered to 1% FDR.

For protein inference, the DIA-NN peptide output was summarized to the gene group level using the 'diann' R package implementation of the MaxLFQ algorithm[10] using a 1% FDR cutoff at both the precursor and gene group level.

Protein groups were filtered to include only those with no missing values in at least one group, and subsequently, missing values were imputed for each protein group from a normal distribution centered around half the minimum observed value for that protein group. Significance was determined by way of ANOVA using the 'aov' function from the default R 'stats' package[11] and defined as those protein groups with $p < 0.05$ after multiple testing correction using the Benjamini–Hochberg method.[12] Data visualizations such as volcano plots, box plots and principal components analysis were rendered using 'ggplot2'[13] and heatmaps using 'pheatmap'.[14]

Enrichment analyses were performed using over-representation analysis of protein groups with significantly altered abundance and gene set enrichment analysis, both conducted via 'clusterProfiler'.[15] Determination of significance for the over-representation analysis was determined in a pairwise fashion between sample groups and defined as having a Benjamini-Hochberg adjusted ANOVA $p < 0.05$, Tukey's posthoc $p < 0.05$,[16] and a fold-change greater than 2 in either direction.

https://doi.org/10.1021/acs.jproteome.5c00889
J. Proteome Res. 2026, 25, 460−470

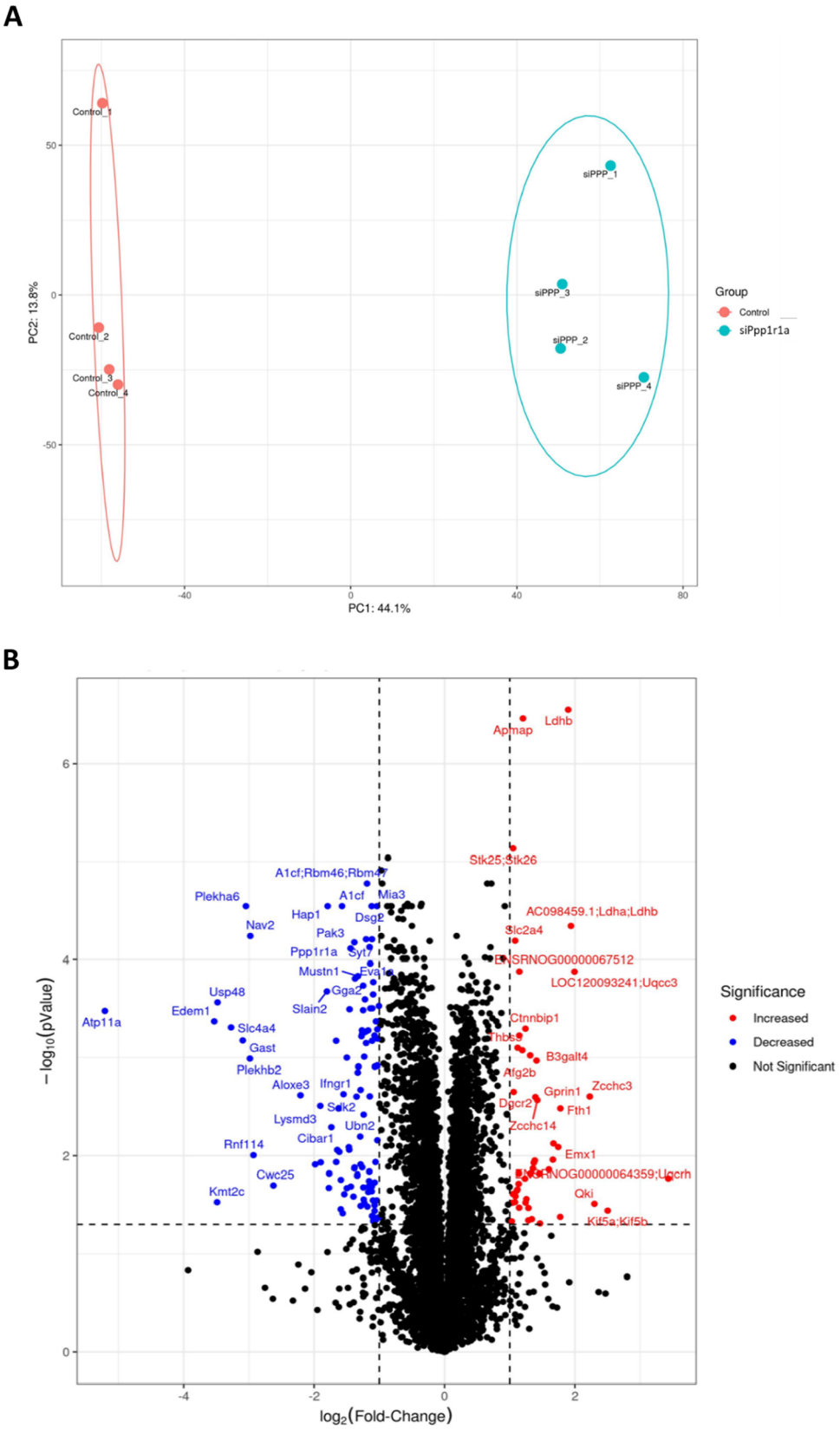

Figure 1. continued

https://doi.org/10.1021/acs.jproteome.5c00889
J. Proteome Res. 2026, 25, 460−470

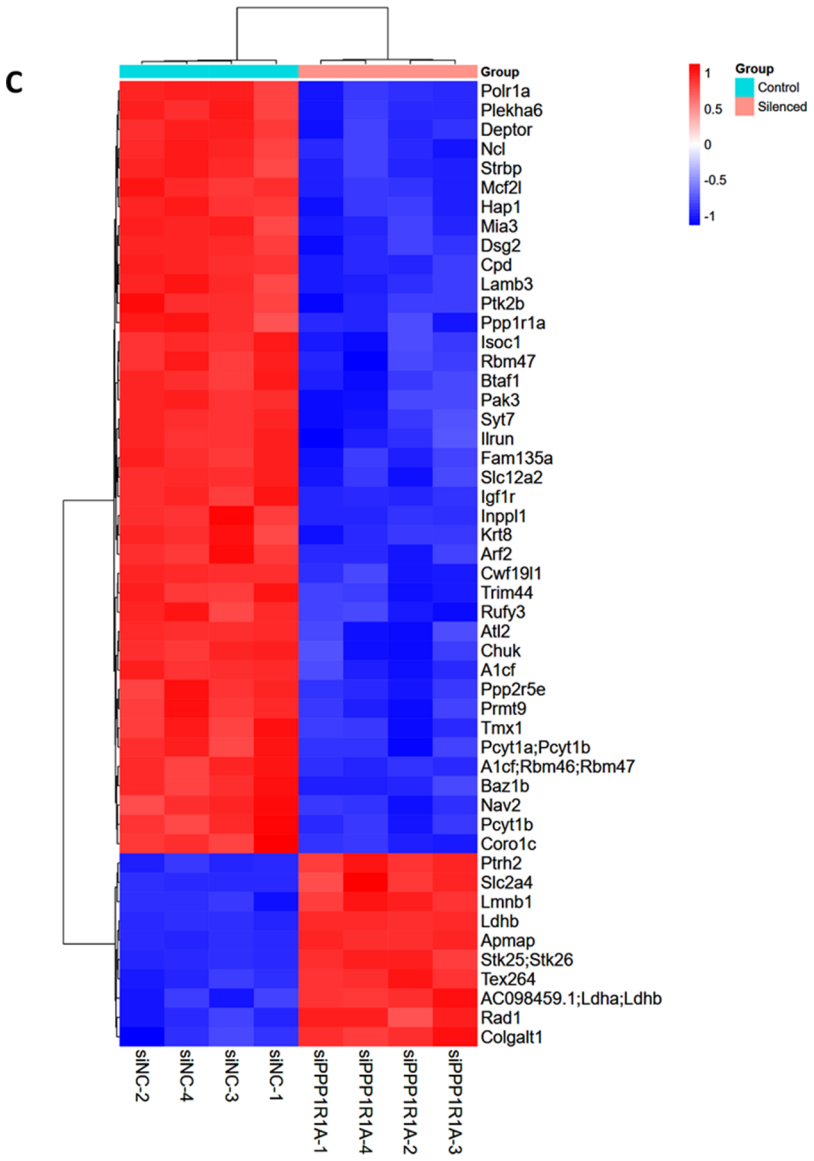

Figure 1. Proteomics analysis of INS-1 cells silenced for Ppp1r1a vs control cells. (A) Principal component analysis (PCA) ($p < 0.05$, Log2FC threshold 1) between Ppp1r1a-silenced INS-1 cells and control cells. Each point represents an individual biological replicate ($n = 4$ per group). The x-axis (PC1) and y-axis (PC2) represent the first and second principal components, respectively, which account for the most significant sources of variance in the data set. The green color indicates Ppp1r1a-silenced cells, and the red color indicates control cells. (B) Volcano plot ($p < 0.05$, Log2FC threshold 1) between Ppp1r1a-silenced INS-1 cells and control cells. The red color indicates the significant upregulated proteins, while the blue color indicates the significant downregulated proteins, while proteins with no significant changes are colored black. (C) Hierarchical clustering analysis (HCA) between Ppp1r1a-silenced cells and control cells. The heatmap displays the relative expression levels, with each row representing an individual protein and each column corresponding to a biological replicate.

Statistical Analysis

All other statistical analyses were performed using GraphPad Prism version 8.0 (GraphPad Software, USA). Statistical significance was defined as a P-value <0.05. Differences between the negative control and Ppp1r1a-silenced cells for immunoblotting experiments were assessed using the Student's t test.

RESULTS

Proteomics Analysis of Ppp1r1a-Silenced INS-1 Cells Revealed Significant Alterations in Protein Expression Compared to Control Cells

PPP1R1A was silenced in INS-1 cells as previously described,[7] with knockdown efficiency (~65%, $p < 0.01$) demonstrated in Figure S1A. This suppression was further confirmed by the current proteomics analysis, as shown in Figure S1B.

Label-free quantitative proteomics was performed to assess the impact of Ppp1r1a silencing on protein expression in Ppp1r1a-silenced samples versus control samples. Principal component analysis (PCA) revealed a robust separation between groups, with the first principal component (PC1) accounting for 44.1% and the second principal component (PC2) accounting for 13.8% of the variance (Figure 1A).

Proteomic profiling quantified a total of 9006 proteins in PPP1R1A-silenced cells. Using a statistical threshold of $p < 0.05$, 2846 proteins were significantly altered, including 1349 upregulated and 1497 downregulated proteins. When applying both statistical significance ($p < 0.05$) and a biological effect-

https://doi.org/10.1021/acs.jproteome.5c00889
J. Proteome Res. 2026, 25, 460−470

Table 1. List of Top 30 Upregulated Proteins in PPP1R1A-Silenced Cells Compared to Control Cells[a]

protein name	Adj-P	P-value	Log2FC	protein description
Ldhb	6.42×10^{-14}	3.15×10^{-11}	1.89679777	L-lactate dehydrogenase B chain
Apmap	6.42×10^{-14}	7.74×10^{-11}	1.203022009	adipocyte plasma membrane-associated protein
Stk25;Stk26	3.26×10^{-10}	2.45×10^{-09}	1.051829127	serine/threonine-protein kinase 26
Ldha	2.23×10^{-07}	1.46×10^{-07}	1.938921	L-lactate dehydrogenase A chain
Slc2a4	3.53×10^{-07}	2.64×10^{-07}	1.082913438	lamin-B1
ENSRNOG00000067512	9.41×10^{-07}	9.51×10^{-07}	1.147468239	glutamyl/glutaminyl-tRNA synthetase class Ib catalytic domain-containing protein
Uqcc3	9.56×10^{-07}	9.67×10^{-07}	1.993189062	ubiquinol-cytochrome-c reductase complex assembly factor 3
Ctnnbip1	1.32×10^{-05}	1.33×10^{-05}	1.240536439	beta-catenin-interacting protein 1
Selenow	1.79×10^{-05}	1.81×10^{-05}	1.146389289	selenoprotein W
Thbs3	3.06×10^{-05}	3.07×10^{-05}	1.121180756	thrombospondin-3
Serpine1	3.34×10^{-05}	3.35×10^{-05}	1.192911488	plasminogen activator inhibitor 1
Afg2b	3.97×10^{-05}	3.98×10^{-05}	1.313794493	ATPase family gene 2 protein homologue B
B3galt4	4.75×10^{-05}	4.76×10^{-05}	1.411121327	beta-1,3-galactosyltransferase 4
Dgcr2	0.000159841	0.000159897	1.060273813	integral membrane protein DGCR2/IDD
Zcchc3	0.000195139	0.000195192	2.227597979	zinc finger CCHC-type containing 3
Gprin1	0.000200388	0.00020044	1.393614048	G protein-regulated inducer of neurite outgrowth 1
Zcchc14	0.000222871	0.000222922	1.423489299	zinc finger CCHC-type containing 14
Fth1	0.000304617	0.000304665	1.776751639	ferritin heavy chain
Dctpp1	0.000996011	0.000996047	1.670799793	uncharacterized protein
Emx1	0.001144583	0.001144617	1.743315022	empty spiracles homeobox 1
Ldhd	0.001807127	0.001807159	1.661632873	probable D-lactate dehydrogenase, mitochondrial
Rbm38	0.001863853	0.001863884	1.384177927	RNA-binding protein 38
Coa4	0.002014353	0.002014384	1.369932853	cytochrome *c* oxidase assembly factor 4 homologue
Rnf7	0.002459858	0.002459888	1.356669542	RING-box protein 2
Fas	0.002535325	0.002535354	1.600553716	tumor necrosis factor receptor superfamily member 6
Trio	0.002878893	0.002878922	1.139904521	triple functional domain protein
Ppt2	0.002909911	0.002909939	1.453606049	lysosomal thioesterase PPT2
Gjd2	0.002911618	0.002911647	1.317682173	gap junction delta-2 protein
Uqcrh	0.003393893	0.00339392	3.432230882	ubiquinol-cytochrome *C* reductase hinge domain-containing protein
Dpp10;Dpp6	0.003419632	0.003419659	1.233244742	A-type potassium channel modulatory protein DPP6

[a]Differentially expressed proteins were filtered by adjusted $P < 0.05$ and classified as upregulated (log2FC > 1).

size cutoff (|Log2FC| > 1), 153 proteins met both criteria, with 48 upregulated (Log2FC > 1, $p < 0.05$) and 105 downregulated (Log2FC < −1, $p < 0.05$). Representative proteins meeting these combined significance and fold-change thresholds are displayed in the volcano plot (Figure 1B).

Hierarchical clustering analysis (HCA) further confirmed distinct proteomic profiles between PPP1R1A-silenced and control cells, with biological replicates clustering tightly within each group (Figure 1C). This suggests that the Ppp1r1a-silenced cells and control cells form distinct subgroups, independent of their biological origin.

Proteins with adjusted *p*-value <0.05 were classified as upregulated (log2FC > 1) or downregulated (log2FC < −1), and ranked in each group by ascending adjusted *p*-value. The top 30 upregulated and top 30 downregulated proteins are shown in Tables 1 and 2, respectively. Notably, among the top 12 most significantly modulated proteins, Rbm46, APMAP, CPD, Cwf19l1, IGF1R, LDHB, Mcf2l, Mia3, Polr1a, Ptrh2, Stk26, and Tex264 emerged as key players potentially involved in the regulatory pathways altered by the silencing of Ppp1r1a. These genes collectively contribute to the intricate network of cellular signaling such as cell growth and signaling (IGF1R),[17] energy metabolism regulation that is important for glucose-stimulated insulin secretion in beta cells (LDHB),[18] ER-to-Golgi protein trafficking and packaging (MIA3, CPD),[19,20] RNA processing and gene expression (Rbm46, Polr1a, Cwf19l1),[21−23] stress and quality control (Tex264),[24] cytoskeletal remodelling (Mcf2l, Stk26),[25,26] and overall beta cell integrity and function (Ptrh2).[27]

Proteomic Pathway Analysis Highlights Insulin Secretion as One of the Top Modulated in Ppp1r1a-Silenced INS-1 Cells

To explore the biological functions associated with the differentially expressed proteins, functional enrichment analyses were performed using Gene Ontology (GO) and Kyoto Encyclopedia of Genes and Genomes (KEGG) pathway databases.

As illustrated by the GO enrichment analysis (Figure 2), the most significantly enriched biological processes were primarily related to intracellular trafficking and vesicle transport, energy metabolism and mitochondrial function, mRNA processing and gene expression regulation, organelle organization and structural regulation, and autophagy and cellular maintenance. This highlights the broad impact of Ppp1r1a silencing on diverse cellular trafficking, metabolic, and regulatory processes in INS-1 cells. Detailed protein-level enrichment data, including significance, enrichment value and protein counts, are provided in Table S1.

KEGG pathway analysis further demonstrated significant enrichment in pathways directly linked to insulin secretion and insulin resistance, underscoring PPP1R1A's pivotal role in *β*-cell function (Figure 3A). This suggests that PPP1R1A knockdown perturbs both secretory machinery and insulin signaling networks within pancreatic *β*-cells. A full list of

https://doi.org/10.1021/acs.jproteome.5c00889
J. Proteome Res. 2026, 25, 460−470

Table 2. List of Top 30 Downregulated Proteins in PPP1R1A-Silenced Cells Compared to Control Cells[a]

protein name	Adj-*P*	*P*-value	Log2FC	protein description
A1cf;Rbm46;Rbm47	1.88×10^{-08}	1.67×10^{-08}	−1.188585899	probable RNA-binding protein 46
Mia3	9.11×10^{-08}	5.64×10^{-08}	−1.035072966	transport and Golgi organization protein 1 homologue
Plekha6	6.60×10^{-08}	4.23×10^{-08}	−3.045686442	pleckstrin homology domain containing A6
Dsg2	9.90×10^{-08}	6.10×10^{-08}	−1.117042288	desmoglein 2
Hap1	7.94×10^{-08}	4.97×10^{-08}	−1.792063519	Huntingtin-associated protein 1
A1cf	1.23×10^{-07}	7.58×10^{-08}	−1.572337013	APOBEC1 complementation factor
Nav2	2.86×10^{-07}	2.00×10^{-07}	−2.9787051	neuron navigator 2
Isoc1	3.27×10^{-07}	2.39×10^{-07}	−1.202821964	isochorismatase domain-containing protein 1
Pcyt1b	3.30×10^{-07}	2.41×10^{-07}	−1.112671656	choline-phosphate cytidylyltransferase B
Pak3	3.77×10^{-07}	2.89×10^{-07}	−1.383212923	serine/threonine-protein kinase PAK 3
Syt7	4.29×10^{-07}	3.45×10^{-07}	−1.149886563	synaptotagmin-7
Ppp1r1a	4.78×10^{-07}	4.00×10^{-07}	−1.440584345	protein phosphatase 1 regulatory subunit 1A
Eva1a	7.84×10^{-07}	7.64×10^{-07}	−1.139427436	Eva-1 homologue A, regulator of programmed cell death
Mustn1	1.17×10^{-06}	1.22×10^{-06}	−1.328452016	musculoskeletal embryonic nuclear protein 1
Gga2	1.30×10^{-06}	1.37×10^{-06}	−1.372421168	Golgi associated, gamma adaptin ear containing, ARF binding protein 2
Pi4k2b	1.54×10^{-06}	1.63×10^{-06}	−1.092644565	phosphatidylinositol 4-kinase type 2-beta
Psme4	1.90×10^{-06}	2.02×10^{-06}	−1.247912624	proteasome activator complex subunit 4
Slain2	2.58×10^{-06}	2.73×10^{-06}	−1.803366928	SLAIN motif family, member 2
Btf3l5;Btf3l7	2.92×10^{-06}	3.08×10^{-06}	−1.094833564	transcription factor BTF3
Rab27a;Rab27b	3.44×10^{-06}	3.61×10^{-06}	−1.219946017	Ras-related protein Rab-27A
Usp48	3.83×10^{-06}	4.00×10^{-06}	−3.481028496	ubiquitin carboxyl-terminal hydrolase 48
P33monox	4.68×10^{-06}	4.86×10^{-06}	−1.005624438	putative monooxygenase p33MONOX
Prkx	5.21×10^{-06}	5.39×10^{-06}	−1.108117389	protein kinase cAMP-dependent X-linked catalytic subunit
Baiap3	5.25×10^{-06}	5.43×10^{-06}	−1.136422873	BAI1-associated protein 3
Sh3gl2	5.44×10^{-06}	5.62×10^{-06}	−1.456687669	endophilin-A1
Ppef2	5.79×10^{-06}	5.96×10^{-06}	−1.248225877	serine/threonine-protein phosphatase with EF-hands
Atp11a	5.96×10^{-06}	6.14×10^{-06}	−5.208615914	phospholipid-transporting ATPase
Edem1	9.33×10^{-06}	9.49×10^{-06}	−3.53189854	alpha-1,2-mannosidase
Polr2m	9.41×10^{-06}	9.57×10^{-06}	−1.051427409	DNA-directed RNA polymerase II subunit GRINL1A
Slc4a4	1.26×10^{-05}	1.28×10^{-05}	−3.273421441	electrogenic sodium bicarbonate cotransporter 1

[a]Differentially expressed proteins were filtered by Adjusted $P < 0.05$ and classified as upregulated (log2FC < −1).

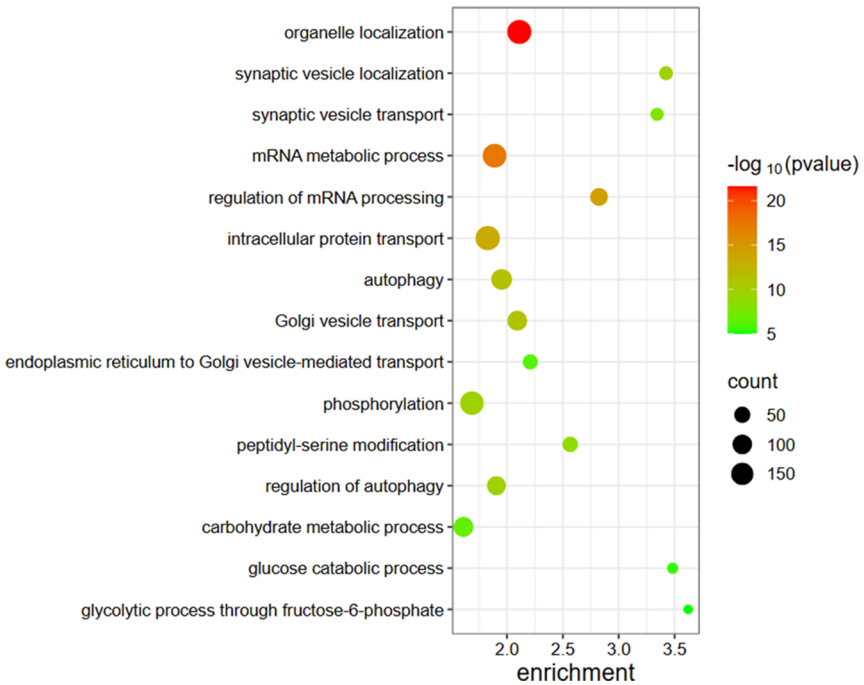

Figure 2. Gene ontology (GO) enrichment analysis. Dot plot illustrating the GO enrichment results for significantly modulated proteins in Ppp1r1a-silenced INS-1 cells. The *x*-axis displays the enrichment score, reflecting the extent of overrepresentation for each GO term among the differentially expressed proteins, while the *y*-axis lists the enriched GO terms. Dot size indicates the number of proteins mapped to each term, and color intensity represents statistical significance ($-\log_{10}$ *p*-value).

https://doi.org/10.1021/acs.jproteome.5c00889
J. Proteome Res. 2026, 25, 460−470

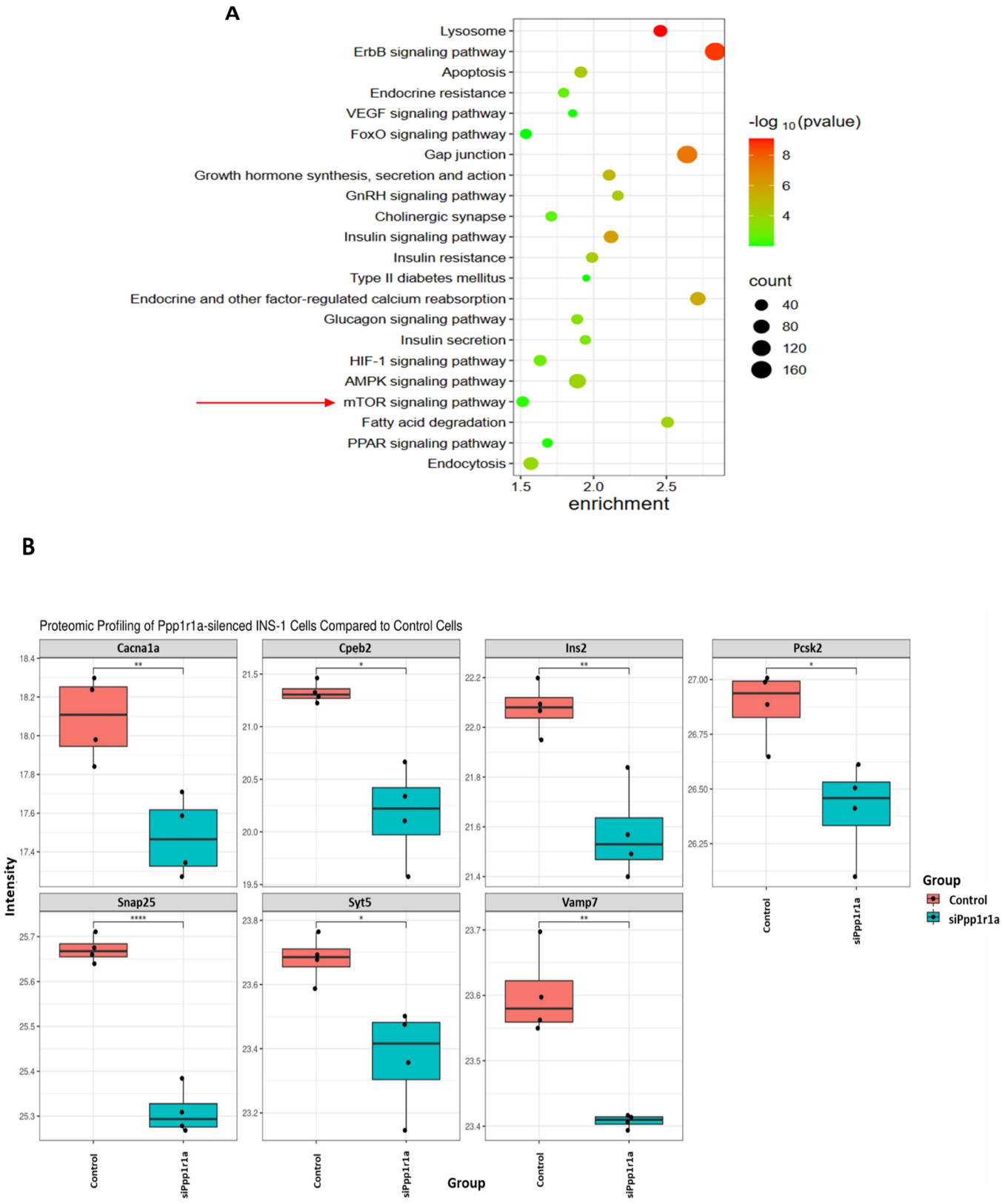

Figure 3. KEGG pathways and protein changes in pancreatic β-cells. (A) Dot plot representing statistically significant enrichment of KEGG pathways ($p < 0.05$) ordered by significance among modulated proteins in Ppp1r1a-silenced INS-1 cells. The x-axis indicates the gene ratio, representing the proportion of proteins from the input data mapped to each pathway, while the y-axis lists the enriched KEGG pathways. Dot size corresponds to the number of modulated proteins assigned to each pathway, and color intensity denotes the level of statistical significance, expressed as the ($-\log_{10}$ of the p-value). (B) Proteomic profiling of Ppp1r1a-silenced INS-1 cells compared to control cells, illustrating relative protein abundance for INS2, Cacna1a, CPEB2, PCSK2, SNAP25, SYT5, and VAMP7. Orange indicates control cells, and green indicates siPPP1R1A-silenced cells. * indicates $p < 0.05$, ** indicates $p < 0.01$, **** indicates $p < 0.0001$.

https://doi.org/10.1021/acs.jproteome.5c00889
J. Proteome Res. 2026, 25, 460−470

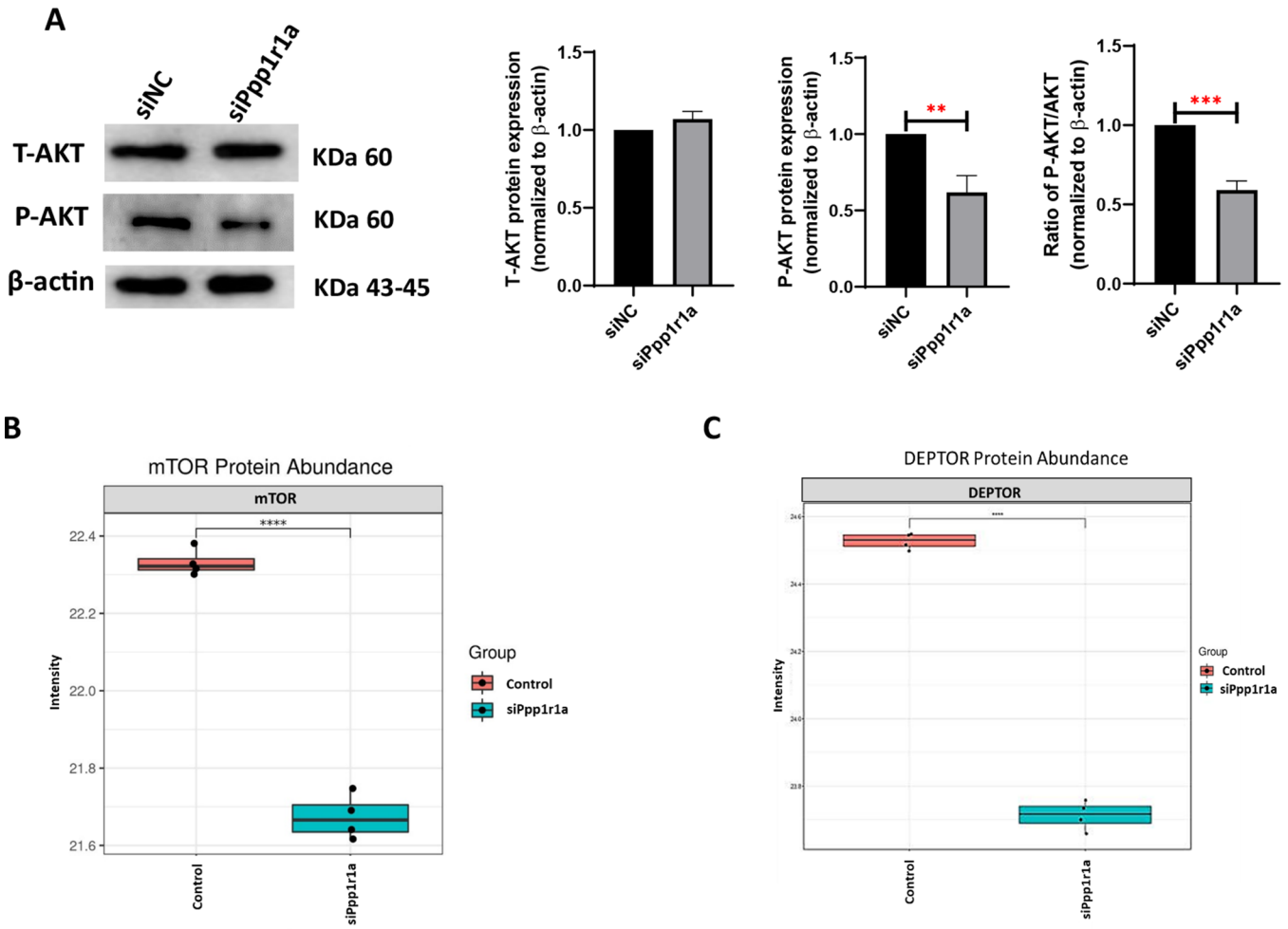

Figure 4. Silencing of Ppp1r1a reduces AKT and p-AKT protein levels. (A) Western blot analysis of Ppp1r1a-silenced INS-1 cells vs control cells showing protein levels of Akt1 and p-Akt. Representative blots are shown alongside densitometric quantification normalized to housekeeping protein (β-actin). Data were obtained from three independent experiments. Uncropped immunoblot images are presented in Supplementary Figure 2. Statistical analysis was performed using Student's t test, with $p < 0.05$ considered statistically significant. ** indicates $p < 0.01$, *** indicates $p < 0.001$. Bars represent ± SD of the mean values. (B) Quantitative proteomic profiling comparing Ppp1r1a-silenced and control INS-1 cells demonstrated a relative decrease in mTOR protein abundance ($p < 0.0001$). (C) Quantitative proteomic profiling comparing Ppp1r1a-silenced and control INS-1 cells demonstrated a relative decrease in DEPTOR protein abundance ($p < 0.0001$).

significantly enriched pathways, along with significance, enrichment value and protein counts, is available in Table S2.

Importantly, Ppp1r1a silencing in INS-1 cells led to a significant reduction ($p < 0.05$) in the abundances of several proteins crucial to β-cell function by means of insulin biosynthesis and secretion, including INS2, Cacna1a, CPEB2, PCSK2, SNAP25, SYT5, and VAMP7 as depicted in Figure 3B.

Ppp1r11 Silencing Attenuates Akt/mTOR Signaling in INS-1 Cells

KEGG pathway analysis revealed that the mTOR signaling pathway was significantly modulated following silencing of Ppp1r1a in INS-1 cells. To gain further mechanistic insight, we examined the expression of key downstream effectors of this pathway, including T-AKT and phosphorylated AKT (p-AKT) (Figure 4A). Our results demonstrated a significant decrease in the protein level of P-AKT ($p < 0.01$), along with a marked reduction in the phosphorylated-to-total AKT ratio ($p < 0.001$) in Ppp1r1a-silenced INS-1 cells compared to controls. Moreover, quantitative proteomic profiling demonstrated a marked decrease in mTOR protein abundance upon Ppp1r1a knockdown ($p < 0.0001$) accompanied by a similarly pronounced decrease in DEPTOR, an endogenous mTOR inhibitor ($p < 0.0001$) (Figure 4B,C). These effects observed upon Ppp1r1a knockdown suggest that PPP1R1A regulates insulin biosynthesis and secretion, at least in part, by modulating the mTOR signaling pathway.

DISCUSSION

Our previous study demonstrated that disruption of PPP1R1A in INS-1 cells leads to impaired insulin secretion and reduced glucose uptake. In contrast, cell viability, oxidative stress (as measured by ROS levels), apoptosis, and proliferation remained unaffected.[7] Notably, transcriptional analyses revealed significant downregulation of key β-cell genes responsible for insulin biosynthesis, processing, glucose sensing, and exocytosis, including Ins1, Ins2, Pcsk1, Cpe, Pdx1, Mafa, Isl1, Glut2, Snap25, Vamp2, Syt5, Cacna1a, Cacna1d, and Cacnb3. In the present study, proteomic profiling of Ppp1r1a-silenced INS-1 cells verified and extended these findings at the protein level. Pathway enrichment analyses highlighted insulin secretion as one of the most significantly perturbed processes in Ppp1r1a-knockdown cells,

https://doi.org/10.1021/acs.jproteome.5c00889
J. Proteome Res. 2026, 25, 460−470

as verified by the marked reduction in the abundance of INS2, Cacna1a, CPEB2, PCSK2, SNAP25, SYT5, and VAMP7 and CPE proteins, which are integral to β-cell insulin biosynthesis and exocytosis. Furthermore, pathway enrichment analysis identified downregulation of the mTOR/Akt signaling axis as a prominent feature following Ppp1r1a silencing, evidenced by decreased levels of p-AKT and phosphorylated-to-total AKT ratio. Collectively, these results indicate that PPP1R1A plays a pivotal role in β-cell function by regulating both the genetic and proteomic landscape governing insulin biosynthesis and secretion, potentially through modulation of the mTOR/Akt signaling pathway.

Previous literature further supports the critical role of PPP1R1A in maintaining pancreatic β-cell functionality and glucose homeostasis. Jiang et al. identified PPP1R1A as a highly abundant and selective protein in β-cells, proposing it as a novel biomarker for β-cell injury with implications for monitoring cell health in both experimental and clinical settings.[28] Their findings emphasize the specificity of PPP1R1A to β-cells and its relevance to the detection of early β-cell damage, underlining its importance in β-cell physiology beyond insulin secretion alone. Additionally, recent mechanistic insights have revealed how chronic cellular stresses impair β-cell adaptive capacity, likely intersecting with regulatory networks involving PPP1R1A, thereby contributing to the progressive dysfunction of β-cells in diabetes.[29] Collectively, these studies complement our previous findings and the current proteomics data, reinforcing the importance of PPP1R1A in β-cell biology and its potential as a target for diabetes treatment.

In a previous study,[6] RNA sequencing analysis of Mafa-deficient mouse islets was performed to uncover novel genes pivotal to β-cell physiology. Among the identified candidates, PPP1R1A emerged as a key regulator essential for glucose-stimulated insulin secretion (GSIS) and for the potentiation of GSIS by glucagon-like peptide-1 (GLP-1). PPP1R1A mediates these effects by modulating mitochondrial bioenergetics and intracellular signaling pathways linked to Gαs-coupled receptors in β-cells. Notably, our current proteomic analysis clearly demonstrates a disruption of the Glucagon signaling pathway and in various intracellular transport and localization signals in Ppp1r1a-silenced INS-1 cells, further supporting the role of PPP1R1A in modulating β-cell incretin responses and amplifying glucose-stimulated insulin secretion.

Our previously published data have demonstrated that PPP1R1A critically regulates several pathways in pancreatic β-cells, most prominently those governing insulin biosynthesis, secretion, and glucose uptake. Disruption or silencing of Ppp1r1a in INS-1 cells results in the downregulation of key genes and proteins involved in insulin processing (e.g., Ins1, Ins2, Pcsk1, Cpe), exocytosis machinery (e.g., Snap25, Vamp2, Syt5), glucose transport (e.g., Glut2), and crucial transcriptional regulators (e.g., Pdx1, Mafa, Isl1), highlighting its role in a network of pathways that maintain β-cell function.[7] Conversely, overexpression of PPP1R1A was found to enhance the expression of insulin, MAFA, PDX1, and GLUT1, affirming its multilevel regulatory function in β-cell physiology. Another previous study reported that exposure of human islets to elevated glucose concentrations for 24 h led to a progressive increase in Ppp1r1a gene expression.[30] Given the established role of PPP1R1A in promoting insulin biosynthesis and secretion, as well as its upregulation under acute high-glucose conditions, sustained decreases in PPP1R1A may impair β-cell insulin output and exacerbate diabetic dysfunction.

Beyond the β-cell context, PPP1R1A is recognized for its regulatory effects on a broader array of signaling networks relevant in health and disease. For instance, in hepatocellular carcinoma (HCC), reduced PPP1R1A expression is correlated with tumor progression and a poor prognosis, with PPP1R1A implicated in modulating the PI3K-Akt signaling axis, cell cycle regulation, and metabolic pathways.[4] Conversely, in Ewing sarcoma, PPP1R1A promotes tumor growth by facilitating cell cycle progression and interacting with the Akt pathway, suggesting a context-dependent regulatory function.[31] Our proteomic profiling identified the mTOR signaling pathway as one of the most significantly modulated following PPP1R1A silencing, which we validated by a reduction in phosphorylated AKT and a decreased p-AKT/AKT ratio, consistent with attenuation of the PI3K−AKT axis. While AKT is classically recognized as a regulator of mTORC1 activity rather than total mTOR abundance,[32] our data also demonstrated a reduction in total mTOR protein levels. Notably, PPP1R1A silencing resulted in a concurrent decrease in DEPTOR, an endogenous inhibitor of mTOR. Under canonical conditions, DEPTOR and mTOR participate in a reciprocal negative feedback loop in which suppression of mTOR typically leads to increased DEPTOR levels.[33] The observed simultaneous reduction in both mTOR and DEPTOR therefore suggests disruption of this regulatory feedback structure.

This coordinated downregulation implies that PPP1R1A may function upstream of the mTOR regulatory network, potentially influencing protein expression stability or turnover mechanisms rather than affecting mTOR solely through AKT-mediated activation. Together, these findings highlight a broader regulatory role for PPP1R1A in maintaining mTOR pathway homeostasis and suggest that PPP1R1A loss shifts signaling dynamics toward a reduced growth and metabolic state.

Our data suggest that sustaining PPP1R1A levels may preserve β-cell insulin secretory capacity, at least partially, through the mTOR pathway. Therefore, PPP1R1A or its downstream effectors could be explored as therapeutic targets for diabetes.

■ ASSOCIATED CONTENT

Data Availability Statement

The mass spectrometry proteomics data generated in this study have been deposited in the ProteomeXchange Consortium via the PRIDE repository under the identifier PXD069033. The data set includes raw mass spectrometry files and processed quantification data.

Supporting Information

The Supporting Information is available free of charge at https://pubs.acs.org/doi/10.1021/acs.jproteome.5c00889.

Figure S1: silencing efficiency of *Ppp1r1a* in INS-1 cells; Figure S2: effect of *Ppp1r1a* silencing on mTOR pathway effectors, uncropped Western blots of AKT and phosphorylated AKT (p-AKT) corresponding to Figure 4, normalized to β-actin, comparing PPP1R1A-silenced and control (siNC) INS-1 cells; Table S1: Gene Ontology (GO) enrichment analysis of *Ppp1r1a*-silenced INS-1 cells compared with control groups; and Table S2: Kyoto Encyclopedia of Genes and Genomes (KEGG) pathway enrichment analysis of *Ppp1r1a*-

https://doi.org/10.1021/acs.jproteome.5c00889
J. Proteome Res. 2026, 25, 460−470

silenced INS-1 cells compared with control groups (PDF)

AUTHOR INFORMATION

Corresponding Authors

Jalal Taneera − *College of Medicine, Department of Basic Medical Sciences and Center of Excellence of Precision Medicine, Sharjah Institute for Medical Research, University of Sharjah, Sharjah 27272, UAE;* orcid.org/0000-0002-3341-1063; Email: jtaneera@sharjah.ac.ae

Eglal Mahgoub − *College of Medicine, Department of Basic Medical Sciences and Research Institute of Medical & Health Sciences, University of Sharjah, Sharjah 27272, UAE;* orcid.org/0000-0001-8314-682X; Email: u20105887@sharjah.ac.ae

Authors

Alexander D. Giddey − *Center for Applied and Translational Genomics (CATG), Mohammed Bin Rashid University of Medicine and Health Sciences (MBRU), Dubai Health, Dubai 505055, UAE;* orcid.org/0000-0002-2034-8122

Nelson C. Soares − *Center for Applied and Translational Genomics (CATG), Mohammed Bin Rashid University of Medicine and Health Sciences (MBRU), Dubai Health, Dubai 505055, UAE; College of Medicine, Mohammed Bin Rashid University of Medicine and Health Sciences, Dubai 505055, UAE; Laboratory of Proteomics, Department of Human Genetics, National Institute of Health, Doutor Ricardo Jorne (INSA), Lisbon 1649-016, Portugal; Comprehensive Health Research Centre (CHRC), NOVA Medical School, University NOVA of Lisbon, Lisbon 1099-085, Portugal;* orcid.org/0000-0003-2331-8532

Anila Khalique − *Research Institute of Medical & Health Sciences, University of Sharjah, Sharjah 27272, UAE*

Abdul Khader Mohammed − *Research Institute of Medical & Health Sciences, University of Sharjah, Sharjah 27272, UAE*

Mohamed Omer Mahgoub − *Department of Health Sciences, College of Natural and Health Sciences, Zayed University, Abu Dhabi 144534, UAE*

Complete contact information is available at: https://pubs.acs.org/10.1021/acs.jproteome.5c00889

Author Contributions

Conceptualization, J.T., supervision, J.T. and N.C.S., methodology, E.M., A.K., M.O.M., and A.G.; writing original draft preparation, E.M. and J.T.; editing, J.T., A.G., A.M., and M.O.M. All authors have read and agreed to the published version of the manuscript.

Funding

J.T. is funded by the College of Research and Graduate Studies, University of Sharjah (No. 22010901117 and 24010901167), MH, UOS Collaborative Research Project No. 2101050170.

Notes

While preparing this work, the author(s) used AI cautiously to improve language and readability. After using this tool/service, the author(s) reviewed the content as needed and took full responsibility for the publication's content.
This research did not involve human or animal participants.
The authors declare no competing financial interest.

REFERENCES

(1) Ferreira, M.; Beullens, M.; Bollen, M.; Van Eynde, A. Functions and therapeutic potential of protein phosphatase 1: Insights from mouse genetics. Biochimica Et Biophysica Acta (BBA)-Molecular. *Cell Research* **2019**, *1866* (1), 16−30.

(2) Taneera, J.; Fadista, J.; Ahlqvist, E.; Atac, D.; Ottosson-Laakso, E.; Wollheim, C. B.; Groop, L. Identification of novel genes for glucose metabolism based upon expression pattern in human islets and effect on insulin secretion and glycemia. *Human molecular genetics* **2015**, *24* (7), 1945−1955.

(3) Chen, J.; Li, Y.; Du, C.; Wei, T.; Shan, T.; Wang, L. Protein kinases in cardiovascular diseases. *Chinese Medical Journal* **2022**, *135* (5), 557−570.

(4) Wu, X.; Wang, Y.; Yang, M.; Wang, Y.; Wang, X.; Zhang, L.; Liao, L.; Li, N.; Mao, M.; Guan, J. Exploring prognostic value and regulation network of PPP1R1A in hepatocellular carcinoma. *Human Cell* **2022**, *35* (6), 1856−1868.

(5) Wittköpper, K.; Fabritz, L.; Neef, S.; Ort, K. R.; Grefe, C.; Unsöld, B.; Kirchhof, P.; Maier, L. S.; Hasenfuss, G.; Dobrev, D. Constitutively active phosphatase inhibitor-1 improves cardiac contractility in young mice but is deleterious after catecholaminergic stress and with aging. *J. Clin. Invest.* **2010**, *120* (2), 617−626.

(6) Cataldo, L. R.; Vishnu, N.; Singh, T.; Bertonnier-Brouty, L.; Bsharat, S.; Luan, C.; Renström, E.; Prasad, R. B.; Fex, M.; Mulder, H. The MafA-target gene PPP1R1A regulates GLP1R-mediated amplification of glucose-stimulated insulin secretion in β-cells. *Metabolism* **2021**, *118*, No. 154734.

(7) Taneera, J.; Mohammed, A. K.; Khalique, A.; Mussa, B. M.; Sulaiman, N.; Bustanji, Y.; Saleh, M. A.; Madkour, M.; Abu-Gharbieh, E.; El-Huneidi, W. Unraveling the significance of PPP1R1A gene in pancreatic β-cell function: A study in INS-1 cells and human pancreatic islets. *Life Sciences* **2024**, *345*, No. 122608.

(8) Doellinger, J.; Schneider, A.; Hoeller, M.; Lasch, P. Sample preparation by easy extraction and digestion (SPEED)-a universal, rapid, and detergent-free protocol for proteomics based on acid extraction. *Molecular & Cellular Proteomics* **2020**, *19* (1), 209−222.

(9) Demichev, V.; Messner, C. B.; Vernardis, S. I.; Lilley, K. S.; Ralser, M. DIA-NN: neural networks and interference correction enable deep proteome coverage in high throughput. *Nat. Methods* **2020**, *17* (1), 41−44.

(10) Cox, J.; Hein, M. Y.; Luber, C. A.; Paron, I.; Nagaraj, N.; Mann, M. Accurate proteome-wide label-free quantification by delayed normalization and maximal peptide ratio extraction, termed MaxLFQ. *Molecular & cellular proteomics* **2014**, *13* (9), 2513−2526.

(11) R Core Team, R. *R: A language and environment for statistical computing*; Citeseer, **2020**.

(12) Benjamini, Y.; Hochberg, Y. Controlling the false discovery rate: a practical and powerful approach to multiple testing. *Journal of the Royal statistical society: series B (Methodological)* **1995**, *57* (1), 289−300.

(13) Villanueva, R. A. M.; Chen, Z. J. *ggplot2: elegant graphics for data analysis*; Taylor & Francis, 2019.

(14) Kolde, R.; Kolde, M. R. *Package 'pheatmap'*; R package, 2015; vol *1*, p 790.

(15) Yu, G. clusterProfiler: An universal enrichment tool for functional and comparative study. *BioRxiv* **2018**, 256784.

(16) Tukey, J. W. Comparing individual means in the analysis of variance. *Biometrics* **1949**, *5*, 99−114.

(17) Kulkarni, R. N. New insights into the roles of insulin/IGF-I in the development and maintenance of β-cell mass. *Reviews in Endocrine and Metabolic Disorders* **2005**, *6* (3), 199−210.

(18) Cuozzo, F.; Viloria, K.; Shilleh, A. H.; Nasteska, D.; Frazer-Morris, C.; Tong, J.; Jiao, Z.; Boufersaoui, A.; Marzullo, B.; Rosoff, D. B. LDHB contributes to the regulation of lactate levels and basal insulin secretion in human pancreatic β cells. *Cell Rep.* **2024**, *43* (4), No. 114047.

(19) Reynolds, H. M.; Zhang, L.; Tran, D. T.; Ten Hagen, K. G. Tango1 coordinates the formation of endoplasmic reticulum/Golgi

docking sites to mediate secretory granule formation. *J. Biol. Chem.* **2019**, *294* (51), 19498−19510.
(20) Kalinina, E. V.; Fricker, L. D. Palmitoylation of carboxypeptidase D: Implications for intracellular trafficking. *J. Biol. Chem.* **2003**, *278* (11), 9244−9249.
(21) Peart, N. J.; Johnson, T. A.; Lee, S.; Sears, M. J.; Yang, F.; Quesnel-Vallières, M.; Feng, H.; Recinos, Y.; Barash, Y.; Zhang, C. The germ cell-specific RNA binding protein RBM46 is essential for spermatogonial differentiation in mice. *PLoS Genet.* **2022**, *18* (9), No. e1010416.
(22) Falcon, K. T.; Watt, K. E.; Dash, S.; Zhao, R.; Sakai, D.; Moore, E. L.; Fitriasari, S.; Childers, M.; Sardiu, M. E.; Swanson, S. Dynamic regulation and requirement for ribosomal RNA transcription during mammalian development. *Proc. Natl. Acad. Sci. U. S. A.* **2022**, *119* (31), No. e2116974119.
(23) Zhang, Y.; Yi, J.; Wei, G.; Ren, T.; Zhao, H.; Zhang, H.; Yang, H.; Zhang, D. CWF19L1 promotes T-cell cytotoxicity through the regulation of alternative splicing. *J. Biol. Chem.* **2024**, *300* (12), No. 107982.
(24) Chino, H.; Hatta, T.; Natsume, T.; Mizushima, N. Intrinsically disordered protein TEX264 mediates ER-phagy. *Mol. Cell* **2019**, *74* (5), 909−921.
(25) Li, M.; Jiao, Q.; Xin, W.; Niu, S.; Liu, M.; Song, Y.; Wang, Z.; Yang, X.; Liang, D. The emerging role of Rho guanine nucleotide exchange factors in cardiovascular disorders: insights into atherosclerosis: a mini review. *Frontiers in Cardiovascular Medicine* **2022**, *8*, No. 782098.
(26) Getu, A. A.; Zhou, M.; Cheng, S.-Y.; Tan, M. The mammalian Sterile 20-like kinase 4 (MST4) signaling in tumor progression: Implications for therapy. *Cancer letters* **2023**, *563*, No. 216183.
(27) Isa, H. M.; Khalaf, S. D.; Janahi, S.; Naser, M. M.; Al Hamad, N.; Alhaddar, H.; Busehail, M. A Novel PTRH2 Gene Mutation Causing Infantile-onset Multisystem Neurologic, Endocrine, and Pancreatic Disease in a Bahraini Patient. *Oman Medical Journal* **2024**, *39* (1), No. e599.
(28) Jiang, L.; Brackeva, B.; Ling, Z.; Kramer, G.; Aerts, J. M.; Schuit, F.; Keymeulen, B.; Pipeleers, D.; Gorus, F.; Martens, G. A. Potential of protein phosphatase inhibitor 1 as biomarker of pancreatic β-cell injury in vitro and in vivo. *Diabetes* **2013**, *62* (8), 2683−2688.
(29) Chen, C.-W.; Guan, B.-J.; Alzahrani, M. R.; Gao, Z.; Gao, L.; Bracey, S.; Wu, J.; Mbow, C. A.; Jobava, R.; Haataja, L. Adaptation to chronic ER stress enforces pancreatic β-cell plasticity. *Nat. Commun.* **2022**, *13* (1), 4621.
(30) Ottosson-Laakso, E.; Krus, U.; Storm, P.; Prasad, R. B.; Oskolkov, N.; Ahlqvist, E.; Fadista, J.; Hansson, O.; Groop, L.; Vikman, P. Glucose-induced changes in gene expression in human pancreatic islets: causes or consequences of chronic hyperglycemia. *Diabetes* **2017**, *66* (12), 3013−3028.
(31) Luo, W.; Xu, C.; Phillips, S.; Gardenswartz, A.; Rosenblum, J. M.; Ayello, J.; Lessnick, S. L.; Hao, H.-X.; Cairo, M. S. Protein phosphatase 1 regulatory subunit 1A regulates cell cycle progression in Ewing sarcoma. *Oncotarget* **2020**, *11* (19), 1691.
(32) Laplante, M.; Sabatini, D. M. mTOR signaling in growth control and disease. *cell* **2012**, *149* (2), 274−293.
(33) Duan, S.; Skaar, J. R.; Kuchay, S.; Toschi, A.; Kanarek, N.; Ben-Neriah, Y.; Pagano, M. mTOR generates an auto-amplification loop by triggering the βTrCP-and CK1α-dependent degradation of DEPTOR. *Molecular cell* **2011**, *44* (2), 317−324.

https://doi.org/10.1021/acs.jproteome.5c00889
J. Proteome Res. 2026, 25, 460−470